Chemical Engineering Journal 155 (2009) 499–507

Contents lists available at ScienceDirect

Chemical Engineering Journal

journal homepage: www.elsevier.com/locate/cej

γ-Ray assisted synthesis of silver nanoparticles in chitosan solution and the antibacterial properties

N.M. Huang[a,*], S. Radiman[b], H.N. Lim[c], P.S. Khiew[d], W.S. Chiu[d], K.H. Lee[e], A. Syahida[e], R. Hashim[a], C.H. Chia[b]

[a] Faculty of Science, University of Malaya, 50603 Kuala Lumpur, Malaysia
[b] School of Applied Physics, Faculty of Science and Technology, Universiti Kebangsaan Malaysia, 43600 Bangi, Selangor Darul Ehsan, Malaysia
[c] Chemistry Department, Faculty of Science, Universiti Putra Malaysia, 43400 UPM Serdang, Selangor Darul Ehsan, Malaysia
[d] Faculty of Engineering and Computer Science, Nottingham University, Jalan Broga, 43500 Semenyih, Selangor Darul Ehsan, Malaysia
[e] Department of Biochemistry, Faculty of Biotechnology and Biomolecular Sciences, Universiti Putra Malaysia, 43400 UPM Serdang, Selangor Darul Ehsan, Malaysia

ARTICLE INFO

Article history:
Received 30 April 2009
Received in revised form 9 July 2009
Accepted 17 July 2009

Keywords:
Nanostructures
Electron microscopy
γ-Ray irradiation
Chitosan
Silver

ABSTRACT

In the present study, chitosan had been utilized as a "green" stabilizing agent for the synthesis of spherical silver nanoparticles in the range of 5–30 nm depending on the percentage of chitosan used (0.1, 0.5, 1.0 and 2.0 wt%) under γ-irradiation. X-ray diffractometer identified the nanoparticles as pure silver having face-centered cubic phase. Ultraviolet–visible spectra exhibited the influence of γ-irradiation total absorbed dose and chitosan concentration on the yield of silver nanoparticles. The antibacterial properties of the silver nanoparticles were tested against Methicillin-resistant *Staphylococcus aureus* (MRSA) (gram-positive) and *Aeromonas hydrophila* (gram-negative) bacteria. This work provides a simple and "green" method for the synthesis of highly stable silver nanoparticles in aqueous solution with good antibacterial property.

1. Introduction

Silver nanoparticles are of great interest amongst the researchers due to their exquisite properties in nanometer size. These particles exhibit potential applications in catalysis, surface enhanced Raman scattering, nanoelectronics, data saving, electromagnetic coating, efficient antibacterial activities [1–6] and the most recent finding reported on the inhibition of the growth of HIV-1 virus [7].

Bacterial pollution on water is a major threat to health. As microorganisms become more resistant to antimicrobial agents [8], there is an increasing need to improve bacteria eradication procedures. The antibacterial properties of silver ions have been recognized for a long time and silver ions have been extensively used as bacteria eradicator in catheter, burn wounds and dental work [9]. Researchers also encourage the use of silver as effective bacteria eradicator for wastes generated from hospitals, which contain highly infectious microorganisms [10,11]. However, remnants of silver ions in treated water might cause adverse effects to health [12]. The emergence of nanoscience and nanotechology in the past few decades has opened the doors of opportunities to study the effect of bacteria eradication using nanoparticles. The antibacterial effect of metal nanoparticles is due to fine metal size and broad surface area to volume, which allows nanoparticles to have intimate contact with membranes of the bacteria and not just based on solubilization of metal ions in solutions [13].

For the last decade, the increased awareness towards the environment has encouraged nanomaterial scientists to look into "greener" methods. The use of non-toxic chemicals, environmental-friendly solvents and renewable resources are important issues in "green" synthesis strategies [14]. Nanomaterials significantly affect the fields of physics, chemistry, electronics, optics, materials science and biomedical science. Even though nanomaterials exhibit special properties due to their size-related effects, their synthesis methods reflect negatively on the environment. Although milder reductants have been introduced for the synthesis of silver nanoparticles such as glucose [15], sodium citrate [16] and polyvinyl pyrrolidone (PVP) [17], most synthesis methods were still highly dependent on the use of toxic chemicals such as sodium borohidride [18], hydrazine [19], formamide [20] and N,N-dimethylformide [21]. These reductants are very reactive, causing environmental and biological risks.

Various methods have been reported for the synthesis of nanosized silver particles e.g. chemical reduction [22–24], photochemical reduction (UV [25], microwave [26,27], electron beam [28] and γ-irradiation [29–32]), micelle [33], reverse micelle [34], microemulsion [35], lamellar liquid crystal [36], aerosol spraying technique [37] and capping agent method [38–40]. Chitosan

* Corresponding author at: Faculty of Science, University of Malaya, 50603 Kuala Lumpur, Malaysia. Tel.: +60 12 2091008; fax: +60 3 58911088.
E-mail address: huangnayming@gmail.com (N.M. Huang).

1385-8947/$ – see front matter © 2009 Elsevier B.V. All rights reserved.
doi:10.1016/j.cej.2009.07.040

is a natural cationic biopolymer consists of D-glucosamine units with excellent bioactivity and biocompatibility. Chitosan has been reported to be used as stabilizer for silver [41], gold [42], metal selenide [43], metal oxide [44] and metal sulfide [45] nanoparticles in the chemical reduction and photochemical reduction methods.

γ-Irradiation reduction method has many advantages in the preparation of metal nanomaterials [46]. The hydrated electrons produced during γ-irradiation can reduce metal ions to metal particles of zero valences [29–32]. This avoids the use of additional reducing agents and the consequent side reactions. Furthermore, the amount of zero-valent nuclei can be controlled by varying the absorbed dose of the irradiation. Homogeneous formation of many nuclei is favorable to result highly dispersed nanoparticles. Hence, it would be interesting to evaluate the morphology of the nanoparticles when synthesized in the chitosan matrix.

In this work, we reported the synthesis of silver nanoparticles by γ-irradiation reduction method with low molecular weight chitosan as stabilizer and co-reductant. Chitosan has been used as stabilizing agent in the synthesis of metal nanoparticles using γ-irradiation method [29,47,48] but the resultant metal nanoparticles have not been tested against antibacterial activity. The chitosan used in this work is a low molecular weight chitosan as compared to high molecular weight chitosan previously used and the γ-irradiation induced reduction of metal nanoparticles took place without the presence of iso-propanol and N_2 atmosphere to make the process simple and more environmental friendly. The resulting nanoparticles were characterized and tested on their efficacy in inhibiting the growth of Methicillin-resistant *Staphylococcus aureus* (MRSA) and *Aeromonas hydrophila* bacteria.

2. Experimental

2.1. Chemical

Silver nitrate dihyrated (98%), acetic acid and low molecular weight chitosan were purchased from Sigma–Aldrich. The molecular weight for chitosan used in this study is approximately 100 kDa. Doubly distilled and deionised water (Purelab Prima Elga, with 18.2 MΩ electrical resistivity) was used throughout the sample preparations. All the chemicals were of analytical grade and were used without further purification.

2.2. Synthesis of silver nanoparticles

Chitosan solutions (20 ml) with concentrations of 0.1, 0.5, 1.0 and 2.0 wt% were prepared by solubilizing chitosan in 1.0 wt% of acetic acid solution (pH ~3.5) under constant stirring for 30 min. Following the usual preparation method of silver nanoparticles, $AgNO_3$ solution (2.0 ml, 0.4 M) was added into the chitosan solution under constant stirring. The chitosan–acetic acid aqueous solution thickened after the addition of $AgNO_3$ solution. The solution which contained silver ions and chitosan was irradiated under γ-irradiation source ^{60}Co with absorbed dosage of 16 and 40 kGy (dose rate at 67 Gy min^{-1} was calibrated using the Fricke dosimetry standard method). The produced silver nanoparticles were yellowish to dark brown, depending on the chitosan concentration and absorbed dosage [49]. Silver nanoparticles were retrieved by centrifugation at 13,000 rpm for 10 min. The supernatant was discarded and the fine precipitate was washed repeatedly for five times using water in order to remove the residue chitosan and reactants.

2.3. Characterizations of silver nanoparticles

The resulting nanoparticles were dried in a vacuum oven at temperature of 60 °C and redispersed in aqueous solution. A drop of the silver nanoparticles solution was deposited onto a carbon-coated copper grid and was allowed to evaporate in the vacuum oven overnight at 60 °C before investigation under a transmission electron microscope (TEM) with an accelerating voltage of 120 kV. The size distribution of the silver nanoparticles was based on diameter of >200 particles on TEM micrographs using I Solution (IMT, Canada) software. Furthermore, dynamic light scattering (DLS) measurements were carried out using a high performance particle sizer (HPPS) supplied by Malvern Instruments and used for particle size measurement. The crystalline phase of the nanoparticles was determined by X-ray diffraction (XRD) using a Philip diffractometer employing a scanning rate of 0.02° s^{-1} in a 2θ range from 10° to 80° with Cu Kα radiation (λ = 1.5418 Å). The ultraviolet–visible (UV–vis) absorption spectra of the nanoparticles were recorded on a PerkinElmer Lambda 35 spectrophotometer in the wavelength range of 200–800 nm using a 10 mm quartz cuvette. All the measurements were carried out at room temperature (25 °C).

2.4. Silver nanoparticles antibacterial efficacy test

Antibacterial efficacy test was carried out on Methicillin-resistant *S. aureus* (MRSA) (gram-positive) and *A. hydrophila* (gram-negative) bacteria using paper disc and liquid LB media method. All the apparatus used in this test were sterilized in an autoclave at 120 °C and pressure of 1 bar for 3 h. For liquid LB media method, silver nanoparticles were added into 50 ml liquid LB medium which was added with 200 μL bacteria at a concentration of 10^7 CFU (colony forming unit). Concentration of silver nanoparticles was determined at 10, 50 and 100 ppm, with 0 ppm as a negative control. The bacteria mixture was left in the incubator-shaker at 37 °C and monitored for 8 h. The mixture was withdrawn hourly for immediate analysis at 600 nm [50] using UV–vis spectroscopy (Thermo Spectronic, Helios Epsilon, USA). UV–vis absorption of 0.1 unit signifies 10^8 CFU bacteria.

3. Results and discussion

A typical XRD pattern of the silver nanoparticles obtained in this work using 1.0 wt% chitosan and 40 kGy of γ-irradiation absorbed dosage is shown in Fig. 1a. The XRD pattern shows four peaks at 38.2°, 44.3°, 64.5°, and 77.3°, which are assigned to the (1 1 1), (2 0 0), (2 2 0) and (3 1 1) planes of face-centered cubic (fcc) silver (JCPDS File No. 04-0783). The absence of silver oxide peaks indicates that the as-prepared nanoparticles are pure silver. The calculated lattice constant, according to the spacing (d_g) of the (1 1 1) plane and the equation $1/d_g^2 = (h_2 + k_2 + l_2)/a^2$ is 0.4089 nm, which is in good agreement with the literature value of 0.4086 nm. The peak at around 21.9° is contributed by the low crystalline soluble chi-

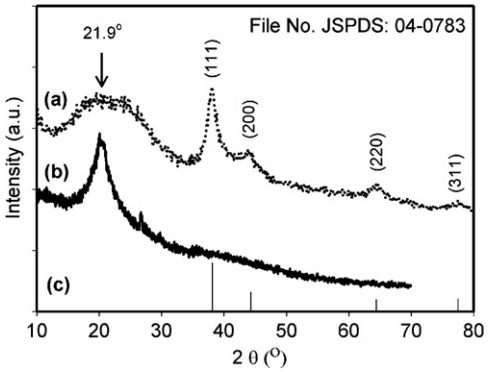

Fig. 1. XRD patterns for (a) silver nanoparticles synthesized in 1.0 wt% low molecular weight chitosan solution under γ-irradiation (40 kGy), (b) low molecular weight chitosan and (c) standard silver (JCPDS 04-0783).

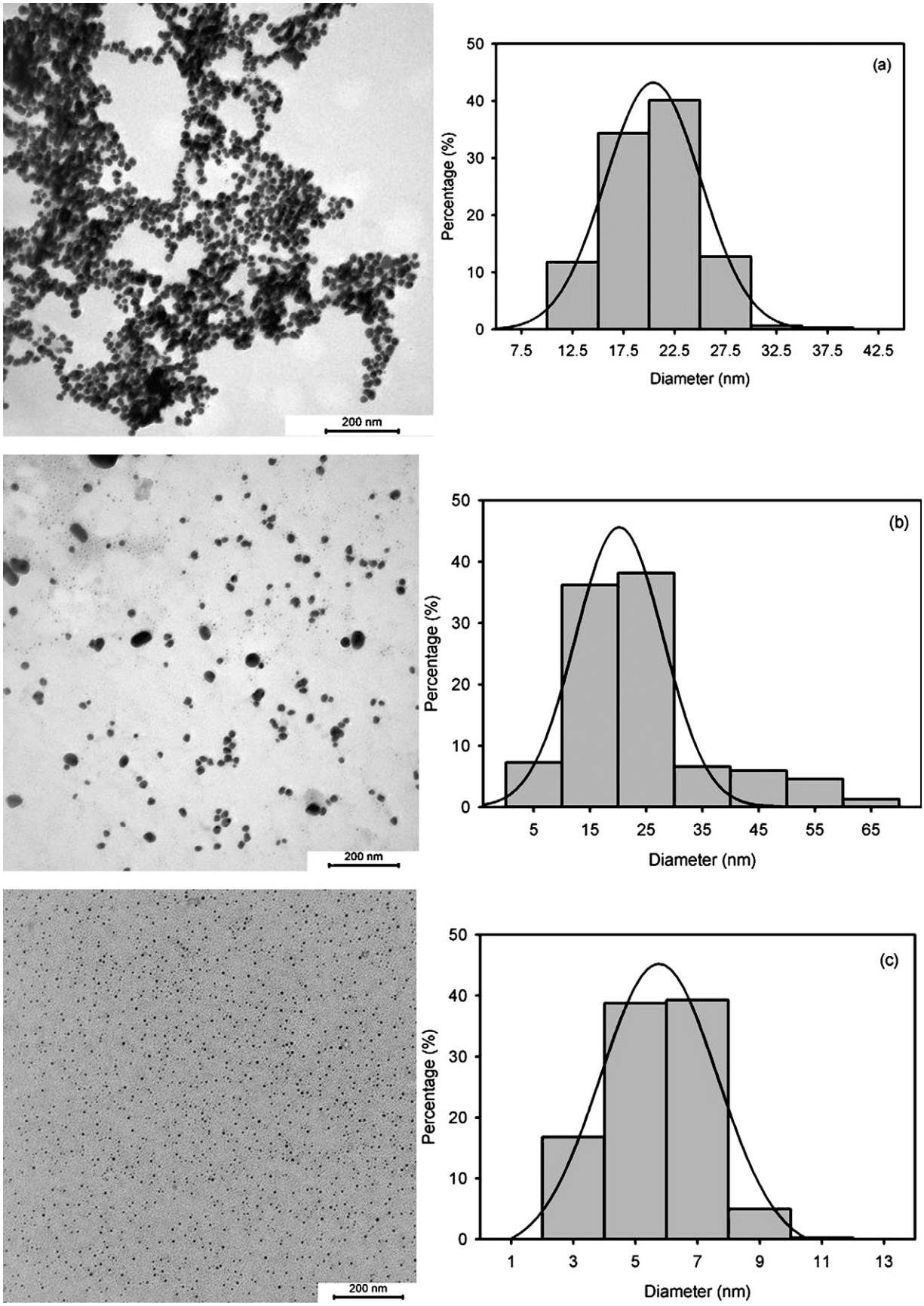

Fig. 2. Silver nanoparticles with chitosan concentrations of (a) 0.1 wt%, (b) 0.5 wt%, (c) 1.0 wt% and (d) 2.0 wt% induced under γ-irradiation absorbed dosage of 16 kGy. Size distribution (diameter) of silver nanoparticles is shown on the right-hand side of the TEM micrographs.

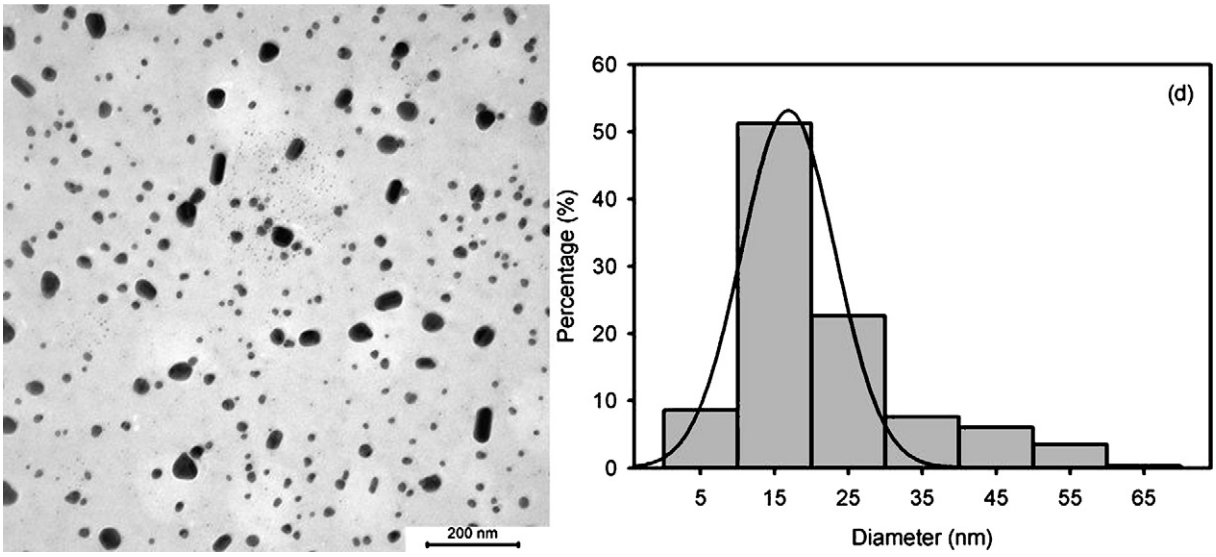

Fig. 2. (*Continued*).

tosan. When comparing this peak with the pure chitosan in Fig. 1b, the pure chitosan has a narrower XRD diffraction peak. The broadening of the chitosan peak in the silver nanoparticles is due to the defragmentation of chitosan polymer under γ-irradiation. Thus, it is evident that the silver nanoparticles are encapsulated by fragments of chitosan.

Silver nanoparticles prepared by γ-irradiation with a total absorbed dose of 16 kGy using different concentrations of chitosan solutions are shown in Fig. 2. From the TEM micrographs, it was observed that chitosan concentration influences the diameter and size distribution of silver nanoparticles. The silver nanoparticles prepared from lower chitosan concentrations of 0.1 and 0.5 wt% had the tendency to aggregate (Fig. 2a and b). Meanwhile, silver nanoparticles prepared from higher chitosan concentrations of 1.0 and 2.0 wt% were segregated uniformly from one another (Fig. 2c and d). This phenomenon is due to the fact that at higher chitosan concentration, >1 wt%, fragments of chitosan produced were sufficient to encapsulate the silver nanoparticles, which prevents them

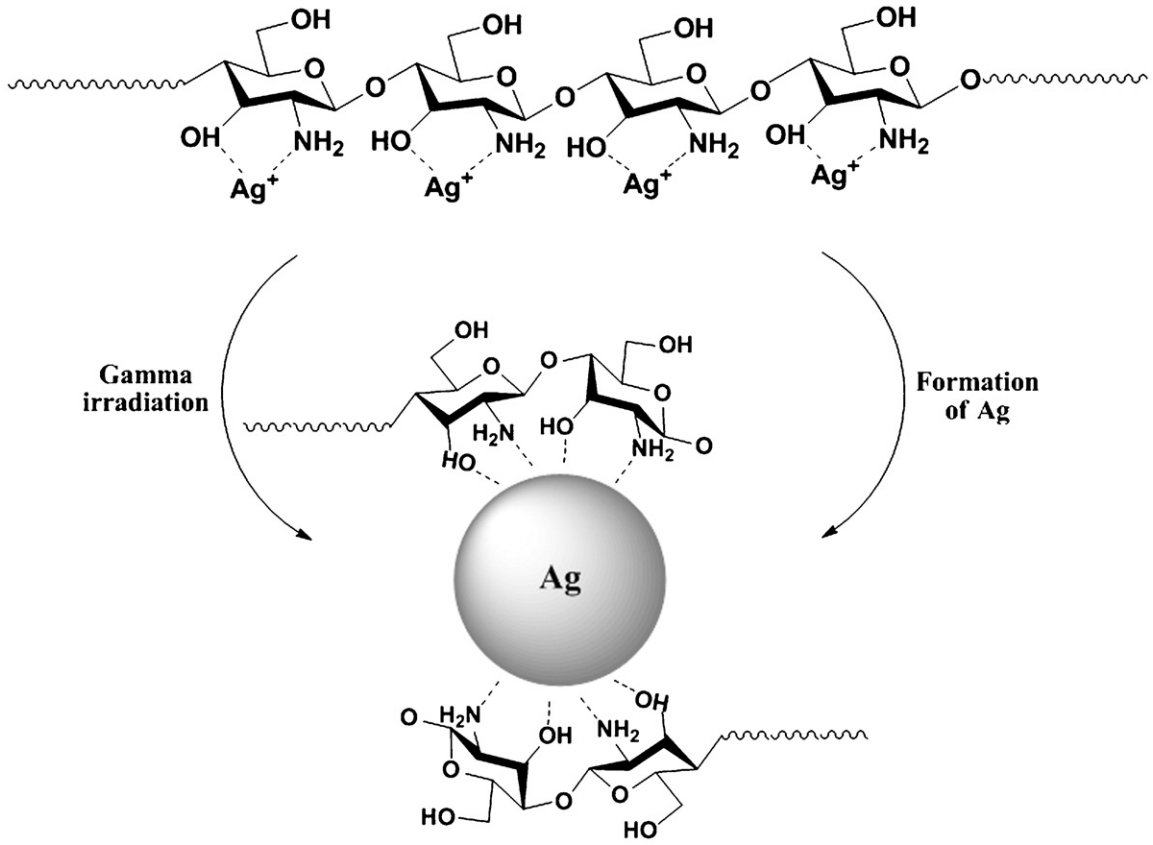

Fig. 3. Schematic mechanism of chitosan fragments encapsulating a silver nanoparticle produced from γ-irradiation reduction.

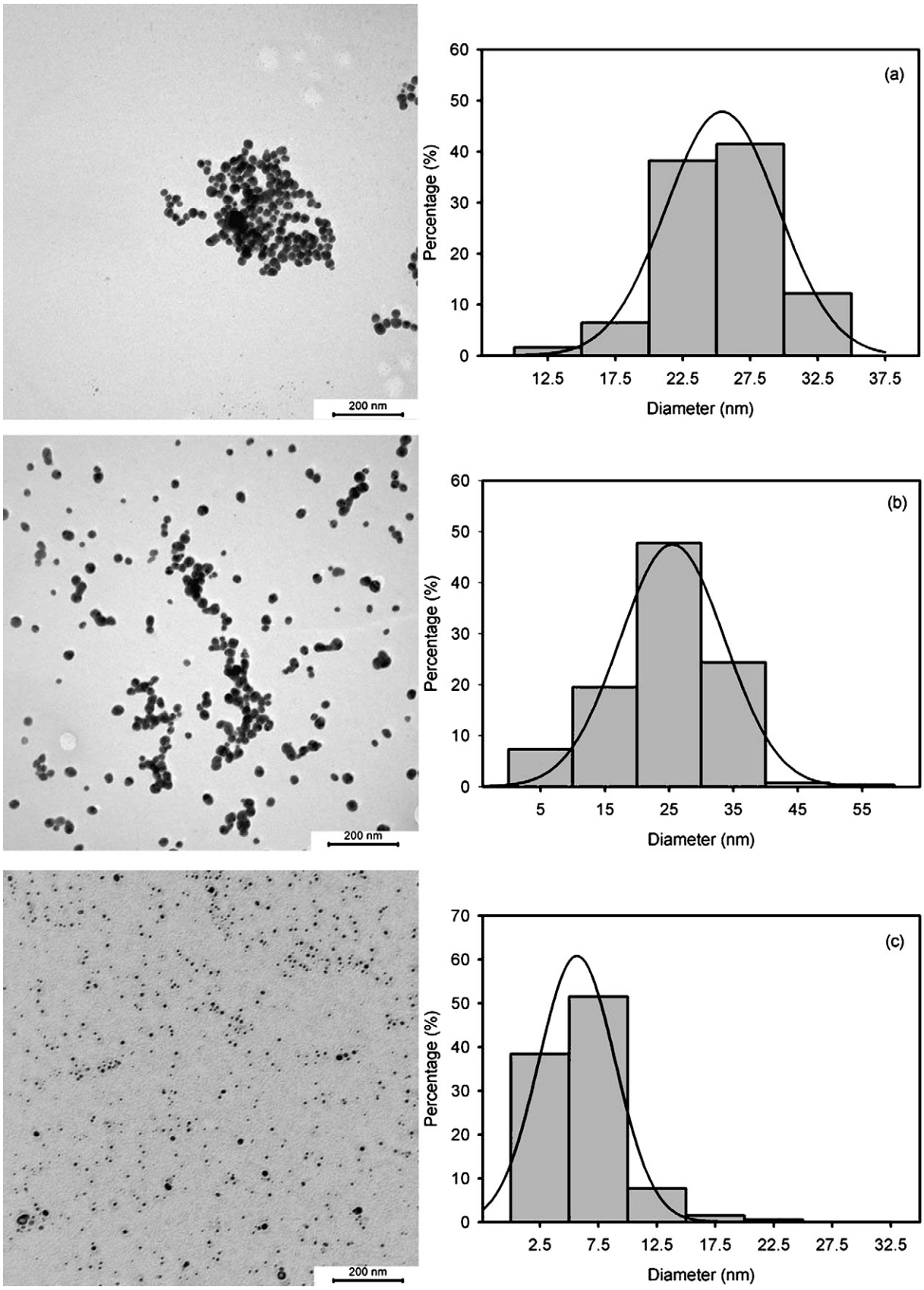

Fig. 4. Silver nanoparticles with chitosan concentrations (a) 0.1 wt%, (b) 0.5 wt%, (c) 1.0 wt% and (d) 2.0 wt% induced under γ-irradiation absorbed dosage of 40 kGy. Size distribution (diameter) of silver nanoparticles is shown on the right-hand side of the TEM micrographs.

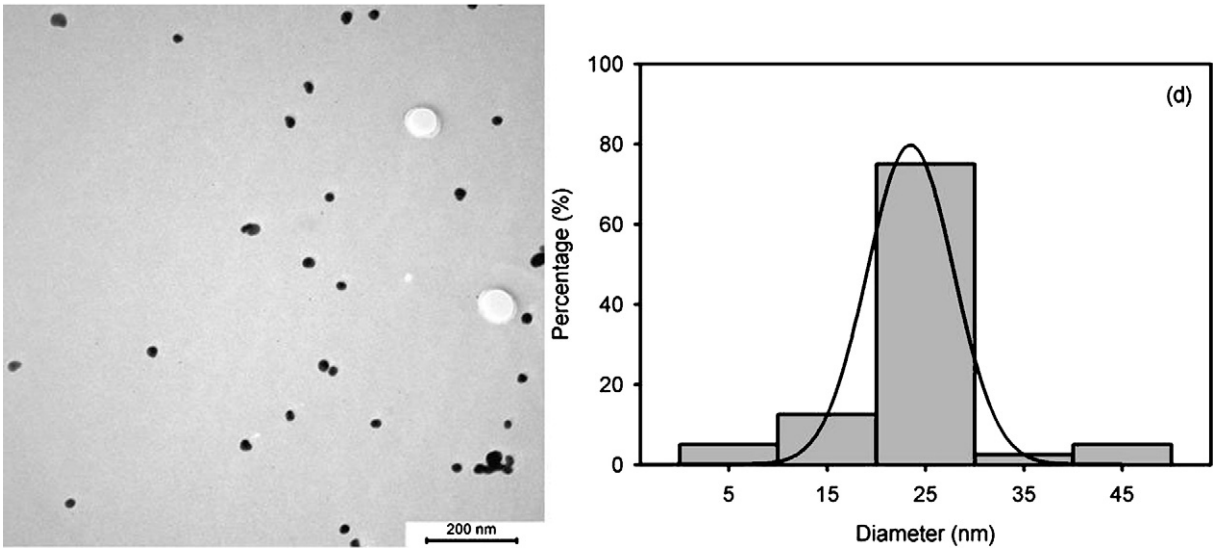

Fig. 4. (*Continued*).

from aggregation. On the other hand, at low chitosan concentration, <0.5 wt%, less fragments of chitosan were produced and thus, unable to hinder aggregation from taking place. The mechanism of chitosan fragments encapsulating a silver nanoparticle produced from γ-irradiation reduction is depicted schematically in Fig. 3. During the γ-ray irradiation, both reduction and defragmentation of chitosan polymer chain happen simultaneously. The reduced silver nanoparticles were capped/stabilized by the presence of fragments of chitosan.

Further TEM micrograph observation shows that the silver nanoparticles produced were spherical and have similar mean diameters of 20.29 ± 4.12 nm for 0.1 wt% chitosan, 23.32 ± 11.97 nm for 0.5 wt% chitosan and 21.40 ± 11.60 nm for 2.0 wt% chitosan (Fig. 2a, b and d). Interestingly, silver nanoparticles prepared from chitosan concentration of 1 wt% have the smallest mean diameter, which is 5.72 ± 1.46 nm (Fig. 2c). It is due to the fact that at lower chitosan concentrations of 0.1 and 0.5 wt%, the amount of chitosan fragments was insufficient to control the particle size of silver nanoparticles. Whereas at higher chitosan concentration of 2 wt%, the viscosity of chitosan solution increased upon addition of $AgNO_3$ solution, which gives rise to gel-like characteristics. The gel-like condition reduced the mobility of radicals, silver ions and silver nuclei in the formation of silver, which promote agglomeration inducing larger particles and causing irregular particle size. Therefore, silver nanoparticles prepared from 2.0 wt% chitosan concentration have broader diameter and size distribution than 1.0 wt% chitosan as shown in the size distribution histogram. The large size distribution for Ag nanoparticles prepared from 2.0 wt% of chitosan is more obvious under prolonged irradiation as shown in Fig. 4d (TEM measurements) and Fig. 5b (DLS).

Fig. 4 shows TEM micrographs and size distribution histograms of silver nanoparticles prepared by γ-irradiation with a total absorbed dose of 40 kGy using different concentrations of chitosan solutions. The mean diameter and standard deviation (representing size distribution) of the silver nanoparticles are 25.45 ± 4.27 nm for 0.1 wt% chitosan (Fig. 4a), 24.59 ± 10.29 nm for 0.5 wt% chitosan (Fig. 4b), 6.31 ± 3.61 nm for 1.0 wt% chitosan (Fig. 4c) and 26.07 ± 19.42 nm for 2.0 wt% chitosan (Fig. 4d). Silver nanoparticles irradiated with absorbed dose of 40 kGy have similar morphology as compared to silver nanoparticles produced from absorbed dose of 16 kGy. Likewise, these nanoparticles are spherical, sensitive to chitosan concentration, have similar patterns of size distribution and affinity to aggregate with each other. The obvious difference is that the silver nanoparticles irradiated with absorbed dose of 40 kGy have larger particle size. This is due to longer period of irradiation resulted in continual growth of silver nanoparticles.

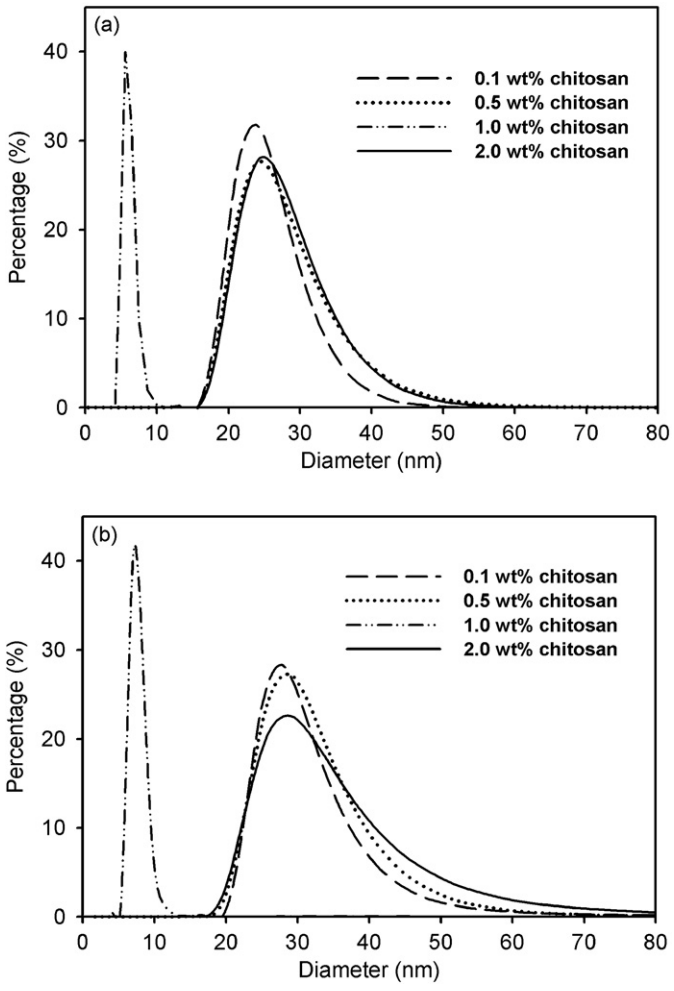

Fig. 5. Dynamic light scattering for Ag nanoparticles synthesized after 16 kGy (a) and 40 kGy (b) of γ-irradiation absorbed dose in various chitosan concentrations.

The size of the Ag nanoparticles produced was further confirmed using dynamic light scattering as shown in Fig. 5. The results are in accord with the TEM observation with Ag nanoparticles synthesized in 1.0 wt% chitosan having the smallest diameter and narrowest size distribution for both 16 kGy (6.02 ± 0.85 nm) and 40 kGy (7.55 ± 1.11 nm) of absorbed dosage. For 0.1, 0.5 and 2.0 wt% of chitosan under 16 kGy of irradiation absorbed dosage, the average diameter were 25.08 ± 4.82, 26.88 ± 6.35 and 26.91 ± 5.94 nm (Fig. 5a). Prolonging the irradiation to 40 kGy resulted in Ag nanoparticles with diameter of 29.67 ± 7.55, 28.6 ± 7.62 and 29.71 ± 11.21 nm for 0.1, 0.5 and 2.0 wt% of chitosan concentrations, respectively (Fig. 5b). The DLS measured size is slightly bigger as compared to the particle size measured from the TEM micrographs because dynamic light scattering method measures the hydrodynamic radius which takes the chitosan coating on the surface of Ag into consideration thus, making the particles bigger [51].

UV–vis spectra of silver nanoparticles (Fig. 6) have characteristic surface plasma absorption peak at around 410–416 nm, resulted from the known Mie scattering [52] which arises from the coherent existence of free electrons in the conduction band due to the small particle size [53]. It was found that the absorption peak for silver nanoparticles with 1.0 wt% chitosan is 410 nm while there is a "red" shift to approximately 416 nm for 0.1 wt%, 0.5 wt% and 2.0 wt% chitosan. This shows that silver nanoparticles with 1.0 wt% chitosan have the smallest particle size [54] which is in accord with the TEM micrographs and DLS measurements. The peak of each spectrum is symmetry, without obvious absorption in the range of 500–800 nm, which suggests the absence of obvious nanoparticles aggregation and that the nanoparticles are generally well segregated [41].

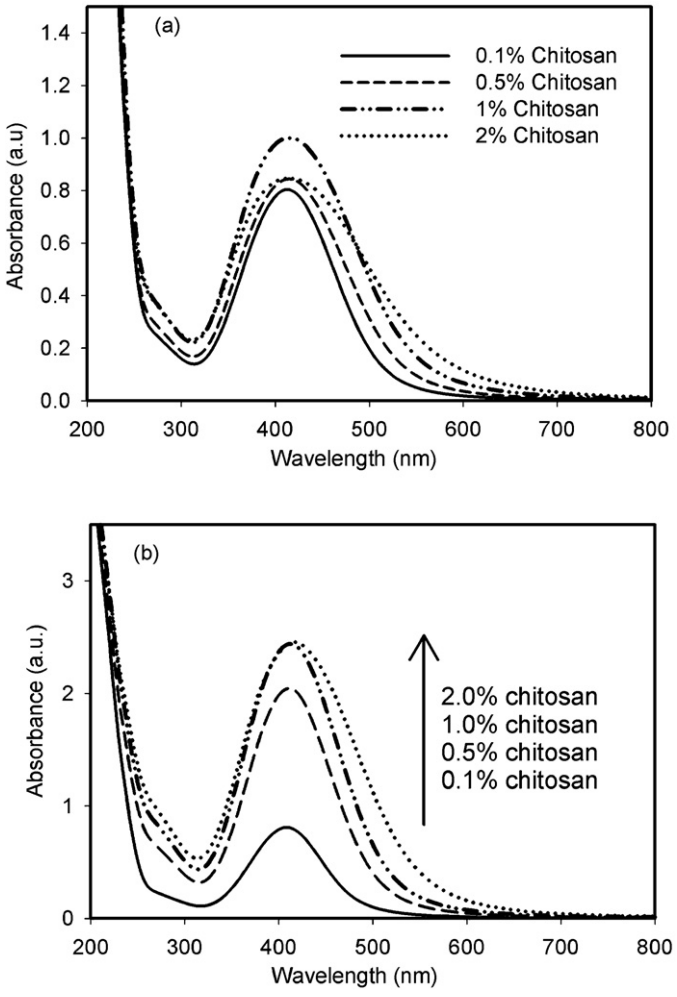

Fig. 6. UV–vis spectra for silver nanoparticles synthesized in different chitosan concentrations under γ-irradiation with absorbed dosage of 16 kGy (a) and 40 kGy (b).

Table 1
The mean absorbance and yield of the silver nanoparticles synthesized in 20 ml of chitosan solution under 40 kGy of γ-irradiation.

Chitosan concentration (wt%)	0.1 wt%	0.5 wt%	1.0 wt%	2.0 wt%
Absorbance (relative intensity)	0.91	2.03	2.48	2.51
Yield (mg)	30.1	66.4	81.7	81.9

The UV–visible absorbance intensity is rather similar for all the as-prepared silver nanoparticles produced at γ-irradiation absorbed dose of 16 kGy (Fig. 6a), which indicates silver nanoparticles having almost the same quantity or yield were formed. When the absorbed dose was increased to 40 kGy, there is a significant difference in the absorbance intensity for different chitosan concentrations as shown in Fig. 6b. Absorbance intensity for the silver nanoparticles increased from chitosan concentrations of 0.1–1.0 wt% and was plateau at chitosan concentrations of 1.0 and 2.0 wt%. In order to obtain the yield, the silver nanoparticles were centrifuged from each chitosan solution and dried, and the weight of the silver nanoparticles was measured using an analytical balance. The yield (in mg) of silver nanoparticles increased with respect to their UV–vis absorbance as shown in Table 1.

Chitosan concentrations of 1.0 and 2.0 wt% produced higher yield of silver nanoparticles as compared to 0.1 and 0.5 wt% of chitosan even though the initial concentration of silver ions was the same in all the chitosan solutions. This shows that chitosan concentration plays an important role in the reduction of silver nanoparticles. We suggest the following formation mechanism of silver nanoparticles under γ-irradiation in the chitosan medium (Eqs. (1)–(8)). This mechanism is similar with some studies on the irradiation reduction of silver in starch solutions [30]:

$$H_2O \xrightarrow{\gamma} e_{aq}^-, H_3O^+, H^\bullet, {}^\bullet OH, H_2, H_2O_2 \quad (1)$$

$$Ag^+ + [C_6H_{11}O_4N]_n \rightarrow [C_6H_{11}O_4N]_nAg^+ \quad (2)$$

$$[C_6H_{11}O_4N]_nAg^+ + e_{aq}^- \rightarrow [C_6H_{11}O_4N]_nAg^0 \quad (3)$$

$$[C_6H_{11}O_4N]_nAg^0 + Ag^+ \rightarrow [C_6H_{11}O_4N]_nAg_2{}^+ \quad (4)$$

$$[C_6H_{11}O_4N]_nAg_2{}^+ + Ag^0 \rightarrow [C_6H_{11}O_4N]_nAg_m{}^+ \quad (5)$$

$$[C_6H_{11}O_4N]_nAg_m{}^+ + e_{aq}^- \rightarrow [C_6H_{11}O_4N]_nAg_m{}^0 \quad (6)$$

$$[C_6H_{11}O_4N]_n + {}^\bullet OH \rightarrow [C_6H_{11}O_4N]_{n-1}[C_6H_{10}O_5N]^\bullet + H_2O \quad (7)$$

$$[C_6H_{11}O_4N]_nAg_m{}^+ + [C_6H_{11}O_4N]_{n-1}[C_6H_{10}O_4N]^\bullet + H_2O \rightarrow [C_6H_{11}O_4N]_nAg_m{}^0 + [C_6H_{11}O_4N]_{n-1}[C_6H_9O_5N] + H_3O^+ \quad (8)$$

The initial mechanism of the reaction in the γ-irradiation synthesis involves interaction of γ-radiation with solvent water molecules, which leads to the formation of e_{aq}^-, H_3O^+, $H^\bullet$, ${}^\bullet OH$, H_2, H_2O_2, etc. Silver ions (Ag^+) forms complex with chitosan, $[C_6H_{11}O_4N]_n$ in the molecular matrix giving $[C_6H_{11}O_4N]_nAg^+$ (Eq. (2)) due to the presence of high number of hydroxyl groups in chitosan. During the γ-irradiation, these ions are reduced by solvated electrons (e_{aq}^-) produced in the aqueous solution giving $[C_6H_{11}O_4N]_nAg^0$ species (Eq. (3)). These neutral Ag^0 atoms encounter the excess nearby Ag^+ ions and produce $[C_6H_{11}O_4N]_nAg_2{}^+$ species (Eq. (4)), which progressively lead to the formation of $[C_6H_{11}O_4N]_nAg_m{}^0$ clusters (Eqs. (5) and (6)). The reduction of these silver ions to chitosan stabilized nanoparticles $[C_6H_{11}O_4N]_nAg_m{}^0$ is induced by strongly reducing e_{aq}^- and the chitosan radicals $[C_6H_{11}O_4N]_{n-1}[C_6H_{10}O_4N]^\bullet$ (Eq. (8)), formed by H atom abstraction reaction from chitosan chains by hydroxyl radicals, ${}^\bullet OH$ (Eq. (7)). These steps of reactions enable

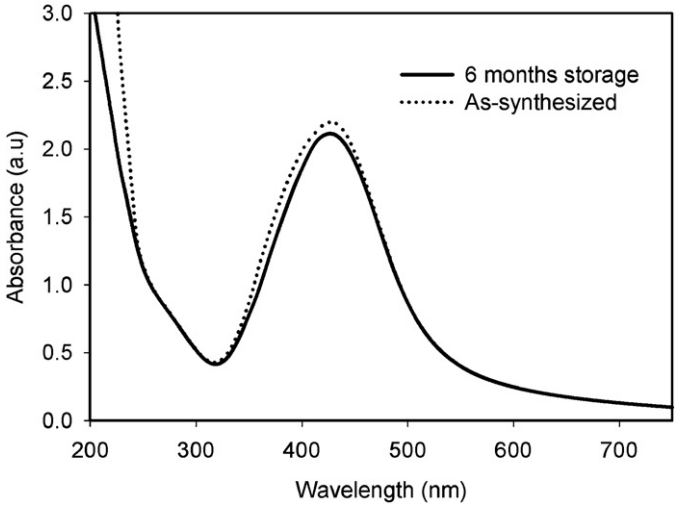

Fig. 7. UV–vis spectra for (a) as-synthesized silver nanoparticles and (b) silver nanoparticles after 6 months of storage in laboratory condition (chitosan concentration of 1 wt% and γ-irradiation absorbed dosage of 40 kGy).

chitosan to reduce Ag^+ ions, coat and stabilize silver nanoparticles while inhibiting their excessive aggregations. Thus, under higher chitosan concentration, the yield of the silver nanoparticles is higher due to the relatively higher amount of chitosan radicals' formed.

The silver nanoparticles synthesized in this work are highly stable. The stability of the chitosan in solution is very important especially in the antibacterial activity as unstable silver particles will not be able to disperse homogenously thus, reducing the antibacterial activity. Fig. 7 shows UV–vis spectra of silver nanoparticles produced using 1.0 wt% chitosan under 40 kGy absorbed dose. Dotted line shows UV–vis spectrum for the as-synthesized silver nanoparticles while solid line represent spectrum for silver nanoparticles after storage of 6 months in laboratory condition. The absence of significant changes on the spectra of the silver nanoparticles after storage suggests high stability of the silver nanoparticles.

The stability of silver nanoparticles in liquid LB media is of high importance because the nanoparticles that are precipitated or aggregated will affect their antibacterial efficacy. Fig. 8 shows the screening of bacterial growth in liquid LB media by measuring the absorbance at 600 nm. Only a small amount of bacterial growth was inhibited by silver at the concentration of 10 ppm as depicted in Fig. 8a. For silver concentration of 50 ppm, the growth of MRSA was inhibited by >50%. Meanwhile, MRSA could not survive in the presence of 100 ppm of silver nanoparticles. When silver nanoparticles were introduced in the medium containing *A. hydrophila* (Fig. 8b), the resistance of the bacteria is higher towards the silver nanoparticles compared to MRSA. The difference in sensitivity is contributed by the nature of the bacteria, in which *A. hydrophila* is a gram-negative bacteria while MRSA is a gram-positive bacteria. Gram-negative bacteria has four layers of protective membranes consisting of a plasma membrane, a periplasmic area, a peptidoglican layer and an outermost layer known as external membrane made-up of protein and lipopolysaccharide. Gram-positive is only enveloped by three layers, which are the plasma membrane, periplasmic area and peptidoglican layer. Therefore, the lack of an extra layer of membrane results in gram-positive bacteria being more sensitive towards the presence of silver nanoparticles. The observation is similar to that of Yoon et al. [55]. At silver concentration of 10 ppm, the inhibition of the bacterial growth is almost negligible whereas the growth was inhibited by <50% at silver concentration of 50 ppm. Nevertheless, the presence of *A. hydrophila* was not detected in the medium comprising

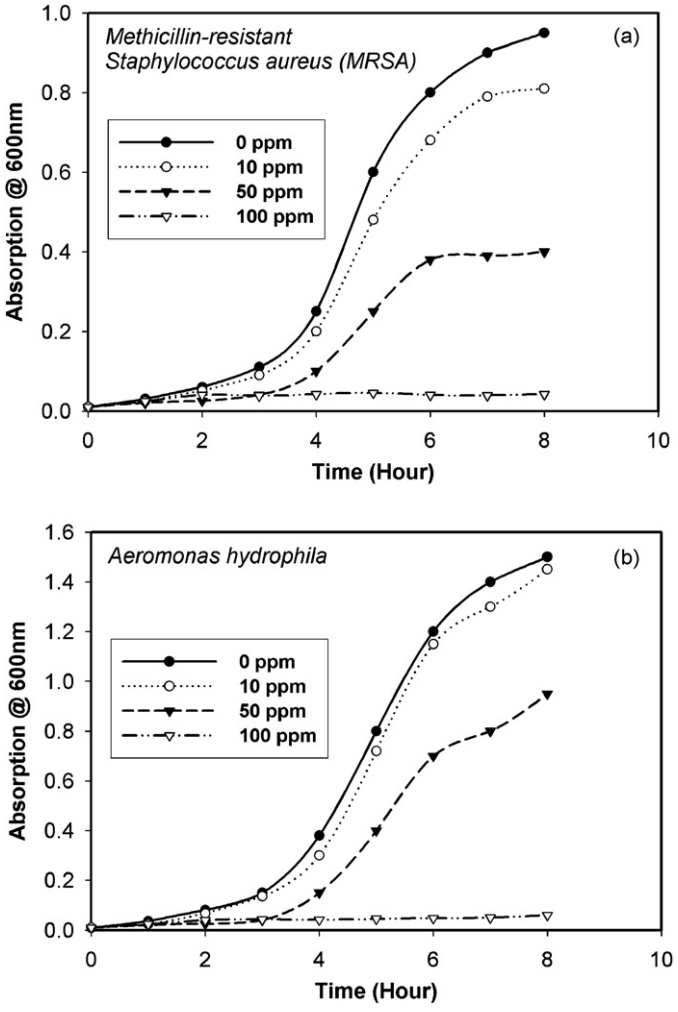

Fig. 8. Silver nanoparticles antibacterial efficacy test using liquid LB media containing (a) MRSA and (b) *Aeromonas hydrophila*.

100 ppm of silver nanoparticles. Based on the antibacterial test, the MIC value of silver nanoparticles is ~100 ppm. This value is similar to the antibacterial activity demonstrated on various bacteria using silver nanoparticles [56,57].

4. Conclusion

This work provides a simple, convenient and "green" method for the synthesis of highly stable silver nanoparticles in chitosan aqueous solution. Silver nanoparticles were successfully synthesized in the presence of low molecular weight chitosan under γ-irradiation without iso-propanol and N_2 atmosphere. Chitosan plays a very important role in the reduction of silver ions (Ag^+) along with γ-irradiation. This is evident as the chitosan concentrations of 1.0 and 2.0 wt% had higher yield of silver nanoparticles than chitosan concentrations of 0.1 and 0.5 wt%. The optimum chitosan concentration was 1.0 wt% with silver nanoparticles having the smallest mean diameter and highest yield. The efficacy of silver nanoparticles in antibacterial activity was manifested on MRSA dan *A. hydrophila*. The MIC value for effective antibacterial activity was ~100 ppm. The simple, cost effective and environmental friendly synthesis of silver nanoparticles using low molecular weight chitosan in addition to their effective antibacterial activity, underlines the potential of adopting this "green" method to produce silver nanoparticles as antibacterial agents for various fields.

Acknowledgements

This work is supported by Universiti Kebangsaan Malaysia through grant no: UKM-OUP-NBT-27-138/2008. The author would like to thank MOSTI for the NSF scholarship.

References

[1] X.Q. Zou, E.B. Ying, S.J. Dong, J. Colloids Interf. Sci. 306 (2007) 307.
[2] L.C. Courrol, F.R. Silva, L. Gomes, Colloids Surf. A 305 (2007) 54.
[3] Y.M. Mohan, K. Lee, T. Premkumar, K.E. Geckeler, Polymer 48 (2007) 158.
[4] X.L. Tian, W.H. Wang, G.Y. Cao, Mater. Lett. 61 (2007) 130.
[5] M.H. Ullah, K. Il, C.S. Ha, Mater. Lett. 60 (2006) 1496.
[6] A. Kameo, T. Yoshimura, K. Esumi, Colloids Surf. A 215 (2003) 181.
[7] J.L. Elechiguerra, J.L. Burt, J.R. Morones, A. Camacho-Bragado, X.X. Gao, H.H. Lara, M.J. Yacaman, J. Nanobiotech. 3 (2005) 6.
[8] M. Kolar, K. Urbanek, T. Latal, Int. J. Antimicrob. Agents 17 (2001) 357.
[9] J.S. Kim, E. Kuk, K. Yu, J. Kim, S. Park, H. Lee, S. Kim, Y. Park, Y. Park, C. Hwang, Nanomed. Nanotech. Bio. Med. 3 (2007) 95.
[10] Y.E. Lin, R.D. Vidic, J.E. Stout, C.A. McCartney, V.L. Yu, Water Res. 32 (1998) 1997.
[11] Y.E. Lin, R.D.S. Vidic, V.L. Yu, Water Res. 30 (1996) 1905.
[12] D.S. Blanc, P. Carrara, G. Zanetti, P. Francioli, J. Hosp. Infect. 60 (2005) 69.
[13] J.R. Morones, J.L. Elechiguerra, A. Camacho, K. Holt, J.B. Kouri, J.T. Ramirez, M.J. Yacaman, Nanotechnology 16 (2005) 2346–2353.
[14] V.K. Sharma, R.A. Yngard, Y. Lin, Adv. Colloids Interf. Sci. 145 (2009) 83.
[15] P. Raveendran, J. Fu, S.L. Wallen, J. Am. Chem. Soc. 125 (2003) 13940.
[16] P.C. Lee, D. Meisel, J. Phys. Chem. 86 (1982) 3391.
[17] H.S. Wang, X.L. Qiao, J.G. Chen, X.J. Wang, S.Y. Ding, Mater. Chem. Phys. 94 (2005) 449.
[18] P.V. Adhyapak, P. Karandikar, K. Vijayamohanan, A.A. Athawale, A.J. Chandwadkar, Mater. Lett. 58 (2004) 1168.
[19] W. Zhang, X. Qiao, J. Chen, H. Wang, J. Colloids Interf. Sci. 302 (2006) 370.
[20] C.R.K. Rao, D.C. Trivedi, Synth. Met. 155 (2005) 324.
[21] I. Pastoriza-Santos, L.M. Liz-Marzan, Langmuir 15 (1999) 948.
[22] P.K. Khanna, N. Singh, S. Charan, V.V.V.S. Subbarao, R. Gokhale, U.P. Mulik, Mater. Chem. Phys. 93 (2005) 117.
[23] B.H. Ryu, Y. Choi, H.S. Park, J.H. Byun, K. Kong, J.O. Lee, H. Chang, Colloids Surf. A 270–271 (2005) 345.
[24] H.S. Wang, X.L. Qiao, J.G. Chen, S.Y. Ding, Colloids Surf. A 256 (2005) 111–115.
[25] S.K. Ghosh, S. Kunda, T. Pal, Bull. Mater. Sci. 25 (2002) 581.
[26] H. Yin, T. Yamamoto, Y. Wada, S. Yanagida, Mater. Chem. Phys. 83 (2004) 66–70.
[27] J. Chen, J. Wang, X. Zhang, Y.L. Jin, Mater. Chem. Phys. 108 (2008) 421.
[28] Y. Li, Y.N. Kim, E.J. Lee, W.P. Cai, S.O. Cho, Nucl. Inst. Meth. Phys. Res. B 251 (2006) 425.
[29] P. Chen, L. Song, Y. Liu, Y. Fang, Radiat. Phys. Chem. 76 (2007) 1165.
[30] M. Kumar, L. Varshney, S. Francis, Radiat. Phys. Chem. 73 (2005) 21.
[31] W.T. Wu, Y. Wang, L. Shi, Q. Zhu, W. Pang, G. Xu, F. Lu, Nanotechnology 16 (2005) 3017.
[32] M.K. Temgire, S.S. Joshi, Radiat. Phys. Chem. 71 (2004) 1039.
[33] C.J. Murphy, N.R. Jana, Adv. Mater. 14 (2002) 80.
[34] M.C. McLeod, R.S. McHenry, E.J. Beckman, C.B. Roberts, J. Phys. Chem. B 107 (2003) 2693.
[35] W.Z. Zhang, X.L. Qiao, J.G. Chen, Chem. Phys. 300 (2006) 495.
[36] L.M. Qi, Y.Y. Gao, J.M. Ma, Colloids Surf. A 157 (1999) 285–294.
[37] L.P. Jiang, A.W. Wang, Inorg. Chem. Commun. 7 (2004) 506.
[38] S. Chen, D.L. Carroll, Nano Lett. 2 (2002) 1003.
[39] A.S. Reddy, C.Y. Chen, S.C. Baker, C.C. Chen, J.S. Jean, C.W. Fan, H.R. Chen, J.C. Wang, Mater. Lett. 63 (2009) 1227–1230.
[40] S.D. Bunge, T.J. Boyle, T.J. Headley, Nano Lett. 3 (2003) 901.
[41] H.Z. Huang, X.R. Yang, Carbohydr. Res. 339 (2004) 2627.
[42] Y.K. Twu, Y.W. Chen, C.M. Shih, Powder Technol. 185 (2008) 251.
[43] N.M. Huang, S. Radiman, H.N. Lim, S.K. Yeong, P.S. Khiew, W.S. Chiu, G.H. Mohamed Saeed, K. Nadarajah, Chem. Eng. J. 147 (2009) 399–404.
[44] B. Feng, R.Y. Hong, Y.J. Wu, G.H. Liu, L.H. Zhong, Y. Zheng, J.M. Ding, D.G. Wei, J. Alloys Compd. 473 (2009) 356–362.
[45] H.Y. Ru Jiang, L. Xiao, Y.H. Chang, Y.J. Guan, X.D. Li, G.M. Zeng, J. Hazard. Mater., in press, doi:10.1016/j.jhazmat.2009.04.037.
[46] T.H. Li, H.G. Park, S.H. Choi, Mater. Chem. Phys. 105 (2007) 325.
[47] D. Long, G. Wu, S. Chen, Radiat. Phys. Chem. 76 (2007) 1126.
[48] D.M. Cheng, X.D. Zhou, H.B. Xia, H.S.O. Chan, Chem. Mater. 17 (2005) 3578.
[49] P. Barnickel, A. Wokaun, W. Sager, H.F. Eicke, J. Colloids Interf. Sci. 148 (1992) 80.
[50] S. Shrivastava, T. Bera, A. Roy, G. Singh, P. Ramachandrarao, D. Dash, Nanotechnology 18 (2007) 225103.
[51] L. D'Souza, A. Suchopar, R.M. Richards, J. Colloids Interf. Sci. 279 (2004) 458.
[52] T. Hasell, J. Yang, W. Wang, P.D. Brown, S.M. Howdle, Mater. Lett. 61 (2007) 4906.
[53] C. Burda, X. Chen, R. Narayanan, M.A. El-Sayed, Chem. Rev. 105 (2005) 1025.
[54] Y. Xia, N.J. Halas, Mater. Res. Soc. Bull. 30 (2005) 338–343.
[55] K. Yoon, J.H. Byeon, J. Park, J. Hwang, Sci. Total Environ. 373 (2007) 572.
[56] J.P. Ruparelia, A.K. Chatterjee, S.P. Duttagupta, S. Mukherji, Acta Biomater. 4 (2008) 707.
[57] I. Sondi, B. Salopek-Sondi, J. Colloids Interf. Sci. 275 (2004) 177.